CrossMark

ORIGINAL ARTICLE

Multi-GNSS precise point positioning with raw single-frequency and dual-frequency measurement models

Yidong Lou[1] · Fu Zheng[1] · Shengfeng Gu[1] · Charles Wang[2] · Hailin Guo[1] · Yanming Feng[2]

Abstract The emergence of multiple satellite navigation systems, including BDS, Galileo, modernized GPS, and GLONASS, brings great opportunities and challenges for precise point positioning (PPP). We study the contributions of various GNSS combinations to PPP performance based on undifferenced or raw observations, in which the signal delays and ionospheric delays must be considered. A priori ionospheric knowledge, such as regional or global corrections, strengthens the estimation of ionospheric delay parameters. The undifferenced models are generally more suitable for single-, dual-, or multi-frequency data processing for single or combined GNSS constellations. Another advantage over ionospheric-free PPP models is that undifferenced models avoid noise amplification by linear combinations. Extensive performance evaluations are conducted with multi-GNSS data sets collected from 105 MGEX stations in July 2014. Dual-frequency PPP results from each single constellation show that the convergence time of undifferenced PPP solution is usually shorter than that of ionospheric-free PPP solutions, while the positioning accuracy of undifferenced PPP shows more improvement for the GLONASS system. In addition, the GLONASS undifferenced PPP results demonstrate performance advantages in high latitude areas, while this impact is less obvious in the GPS/GLONASS combined configuration. The results have also indicated that the BDS GEO satellites have negative impacts on the undifferenced PPP

performance given the current "poor" orbit and clock knowledge of GEO satellites. More generally, the multi-GNSS undifferenced PPP results have shown improvements in the convergence time by more than 60 % in both the single- and dual-frequency PPP results, while the positioning accuracy after convergence indicates no significant improvements for the dual-frequency PPP solutions, but an improvement of about 25 % on average for the single-frequency PPP solutions.

Keywords Multi-GNSS · PPP · MGEX · Convergence time

Introduction

In recent years, the realm of global satellite navigation has experienced dramatic changes. GPS is introducing modernized signals, there have been eight BLOCK IIF satellites transmitting L5 signals, and the BLOCK IIF-9 satellite was successfully launched on March 25, 2015. As the second operational global navigation system, GLONASS has launched a GLONASS-K1 flight-test satellite on November 30, 2014, in which a civil CDMA signal has been transmitted in the GLONASS L3 band (1207.14 MHz). Independently, the BeiDou Navigation Satellite System (BDS) deployed by China has been providing official navigation service for the Asia Pacific area since the end of 2012. Its current constellation consists of five Geostationary Orbiters (GEO), five Inclined Geosynchronous Orbiters (IGSO), and four Medium altitude Earth Orbiter (MEO) satellites (Yang et al. 2011). Meanwhile, Europe has launched four Galileo In-Orbit Validation (IOV) satellites, which transmit signals with superior noise and multipath performance by employing the Alternate Binary Offset Carrier (AltBOC)

✉ Shengfeng Gu
 gsf@whu.edu.cn

1 GNSS Research Center, Wuhan University, Luoyu Road 129, Wuhan 430079, Hubei, China

2 Science and Engineering Faculty, Queensland University of Technology, George St, Brisbane, QLD 4000, Australia

Springer

modulation. The Full Operational Capability (FOC) phase has started with two FOC satellites launched on August 22, 2014, into the wrong orbit. The third and fourth FOC satellites were successfully launched on March 27, 2015.

To prepare for incorporation of the new and modernized systems, the International GNSS Service (IGS, Dow et al. 2009) initiated the Multi-GNSS Experiment (MGEX) in 2012. Various IGS Analysis Centers (ACs) and researchers have routinely provided precise satellite orbit and clock products for BDS (Zhao et al. 2013), Galileo (Hackel et al. 2013), QZSS (Steigenberger et al. 2013) in addition to GPS and GLONASS, based on the MGEX stations. The Galileo precise orbit solutions generated by the Technische Universität München (TUM) and CNES/Collect Localization Satellites (CLS) have demonstrated a precision of one decimeter (Steigenberger et al. 2015). Similar results have been achieved for BDS precise orbit solution with the PANDA software by Wuhan University (Zhao et al. 2013; Lou et al. 2014). The GFZ (Geoforschungszentrum) also provides BDS precise orbits and clocks (http://www.igs.org/mgex/products). Apart from the orbit and clock products, the differential code biases (DCB) for GPS, GLONASS, BDS, and Galileo have been estimated using the MGEX multi-GNSS observation data and Global Ionosphere Maps (Montenbruck et al. 2014).

In addition to generating precise orbit, clock, and DCB products, extensive research efforts have been focused on utilizing multi-GNSS observation data to accelerate the PPP initialization time and positioning performance. The early results of combined GPS/GLONASS PPP solutions obtained by Cai and Gao (2007) did not show significant improvement in convergence time, probably due to the limited number of GLONASS satellites available at that time. Being attributed to the space segment upgrade, more in-depth studies concerning GLONASS and GPS/GLONASS data processing have been published in the following years. In Cai and Gao (2013), a combined GPS/GLONASS PPP model was developed, which is based on the ionospheric-free combination. The results indicated that the combined GPS/GLONASS PPP approach improved the convergence time significantly when compared to the GPS-only PPP. However, all of the testing stations are located in the high latitude region and the inter-frequency biases (IFB) of the GLONASS satellites that reached up to 25 ns were not considered (Defraigne and Baire 2011). Chuang et al. (2013) has pointed out the importance of the receiver IFB of GLONASS in PPP, and the results have demonstrated that the mean RMS of GLONASS-only PPP is improved by almost 50 % during the convergence period. In recognition of the rapid development of BDS, Ge et al. (2012) carried out BDS PPP in both static and kinematic modes and indicated that accuracy at the centimeter level can be obtained. Based on PANDA, Li et al. (2014)

realized the combination of BDS/GPS PPP, showing that kinematic BDS/GPS PPP improves the convergence time and accuracy significantly compared to those of BDS-only and GPS-only kinematic PPP. However, this is based on results from a single station.

It is also noted that the above studies are all based on the ionospheric-free model, namely IF-PPP. However, the IF-PPP approach is originally formulated for dual-frequency observations and is not necessarily the best approach in the multi-GNSS and multi-frequency environment (Schönemann et al. 2011).

Another approach is to directly use the undifferenced or raw observation models in PPP processing. For this approach, the individual signals for each frequency are treated as independent observables, thus avoiding noise amplification in the linear combinations (Le and Tiberius 2007). Additionally, the ionospheric delay is estimated as parameters which can potentially improve the positioning performance by employing an a priori ionosphere model (Shi et al. 2012; Gu et al. 2015). PPP based on raw observations provides an alternative solution to the future multi-frequency GNSS data analysis. This concept has been adopted by Tu et al. (2013) and has demonstrated the advantage of GPS + GLONASS PPP over the GPS-only PPP solutions. The same concept was also adopted by Monge et al. (2014) in the MAP3 algorithm in a two-step manner: The smoothed pseudoranges, initial phase ambiguities, and slant ionospheric delay are estimated in the first step and then corrected in the absolute position estimation. There is also a one-step approach in which all available observables are incorporated in an integrated adjustment (Schönemann et al. 2011). However, the above studies were carried out with an insufficient number of satellites, and less-precise ephemeris products may have affected the results. With the rapid development of GNSS systems and the availability of GNSS precise products, it becomes possible to more comprehensively evaluate the multi-GNSS PPP performances in a much wider scope and give a more complete picture.

This study exploits the contribution of multi-GNSS to single-frequency and dual-frequency PPP solutions based on raw observations. With the raw observation models for code and phase signals, a general observational model independent of the navigation systems is presented first. The model is designed to be not only applicable for CDMA signals transmitted by GPS, BDS, and Galileo, but also applicable for FDMA signals transmitted by GLONASS. Next, the PPP results based on raw observations are evaluated with the global 105 MGEX stations for the whole month of July 2014. The performance is mainly evaluated in terms of convergence time and the positioning accuracy of the PPP with raw single- and dual-frequency data in various multi-GNSS constellation configurations. The

performance is compared with the conventional IF-PPP approach, mainly with the GPS constellation. The regional effects of GLONASS at different latitudes on the PPP approach are also examined. The impacts of the inclusion of BDS GEO satellites are also investigated. Finally, the multi-GNSS PPP performance is analyzed with raw single-frequency and dual-frequency data processing.

Multi-GNSS PPP observation models

Compared to the traditional IF-PPP models, additional unknown parameters such as ionosphere and the time delay biases are included in the PPP models. Referring to modeling of ionosphere in Shi et al. (2012), we focus on the processing strategy of using time delay biases for different GNSS systems. The bias in GLONASS IF-PPP models is also considered.

Function models of multi-GNSS PPP

The basic observations of the GNSS pseudorange and carrier phase are generally expressed as follows (Schönemann et al. 2011):

$$\left.\begin{aligned} \Delta P_{r,f}^s &= u_r^{sT}\Delta x_r^s + t_{r,sys} - t_f^s + b_{r,f} - b_f^s + \beta_{r,f}^s \Delta I_{z,r}^s + \varepsilon_P \\ \Delta \Phi_{r,f}^s &= u_r^{sT}\Delta x_r^s + t_{r,sys} - t_f^s + b_{r,f} - b_f^s - \beta_{r,f}^s \Delta I_{z,r}^s - \lambda_f \Delta N_{r,f}^s + \varepsilon_L \end{aligned}\right\} \quad (1)$$

where $\Delta P_{r,f}^s$ and $\Delta \Phi_{r,f}^s$ are the observed-minus-computed pseudorange and carrier phase on frequency f for the specific satellite s and receiver r pair in metric units, in which the antenna phase center corrections and the phase windup error are corrected, Δx_r^s contains the user's position increments and the zenith tropospheric delay, and u_r^{sT} is the corresponding coefficient vector after linearization. The symbol u_r^{sT} denotes the receiver clock offset corresponding to the system "sys" (for GPS, GLONASS, BDS, and Galileo), t_f^s is the satellite clock offset for different frequency observations, I_z denotes the zenith total electron content, the scalar $\beta_{r,f}^s = \gamma_r^s \cdot 40.3/f^2$ is the product of the ionosphere mapping function γ_r^s and the frequency-dependent factor, and $b_{r,f}$ and b_f^s are the frequency-dependent signal delays for receiver r and satellite s, respectively. The float ambiguity N expressed in cycle is linked to the phase observable through the wavelength λ. Finally, ε_P and ε_L are the measurement noise of pseudorange and carrier phase, respectively.

Considering that the user antenna r is tracking j satellites with n frequencies, from the basic Eq. (1) the observation equation for GNSS PPP can be written as

$$l = AX + v \quad (2)$$

When using undifferenced or raw observations in PPP,

$$\begin{aligned} l = \big(\Delta P_{r,1}^1 \quad \cdots \quad \Delta P_{r,n}^1 \quad \Delta \Phi_{r,1}^1 \quad \cdots \quad \Delta \Phi_{r,n}^1 \\ \Delta P_{r,1}^2 \quad \cdots \quad \Delta \Phi_{r,n}^2 \quad \cdots \quad \Delta P_{r,n}^j \quad \cdots \quad \Delta \Phi_{r,n}^j \big)^T \quad (3) \end{aligned}$$

$$A = \big(A_u \quad e_{2 \cdot n \cdot j} \quad -\Lambda_j \otimes e_{2 \cdot n} \quad A_b \quad -\Lambda_j \otimes (e_2 \otimes \Lambda_n) \quad A_I \quad A_N\big) \quad (4)$$

where $A_u = \big(u_r^{s1} \quad u_r^{s1} \quad \cdots \quad \cdots \quad u_r^{sj} \quad u_r^{sj} \quad \big)^T$, $e_m = (1 \quad \cdots \quad 1)^T$, is $m \times 1$ with one entries, $\Lambda_m = \mathrm{diag}(1 \quad \cdots \quad 1)$, which is a $m \times m$ identity matrix and

$$A_b = \begin{cases} e_j \otimes (e_2 \otimes \Lambda_n) & \text{CDMA} \\ \Lambda_j \otimes (e_2 \otimes \Lambda_n) & \text{FDMA} \end{cases} \quad (5)$$

$$A_I = \mathrm{diag}\big(\gamma_r^1 \quad \gamma_r^2 \quad \cdots \quad \gamma_r^j\big) \\ \otimes \left((1-1)^T \otimes \left(\frac{40.3}{f_1^2} \quad \frac{40.3}{f_2^2} \quad \cdots \quad \frac{40.3}{f_n^2}\right)^T\right) \quad (6)$$

$$A_N = \Lambda_j \otimes (\mathrm{diag}(0,1) \otimes \mathrm{diag}(\lambda_1 \quad \cdots \quad \lambda_n)) \quad (7)$$

$$X = \begin{bmatrix} \Delta x_r^s & t_r & t^s & b_r & b^s & \tilde{I} & \tilde{N} \end{bmatrix}^T \quad (8)$$

where $\otimes$ is the Kronecker product.

By introducing the IF transformation $J = \left(\dfrac{f_1^2}{f_1^2 - f_2^2} \quad \dfrac{-f_2^2}{f_1^2 - f_2^2}\right)$ to the dual-frequency observable, i.e., $n = 2$, denoting the linear transformation P_j as

$$P_j = \big(J_1 \quad J_2 \quad \cdots \quad J_j\big) \quad (9)$$

where each J-term for each satellite j is identical to the 1-by-2 IF-transformation vector J defined above, we can write

$$l_{IF} = \big(\Delta P_{r,IF}^1 \quad \Delta \Phi_{r,IF}^1 \quad \Delta P_{r,IF}^2 \quad \Delta \Phi_{r,IF}^2 \quad \cdots \quad \cdots \quad \Delta P_{r,IF}^j \quad \Delta \Phi_{r,IF}^j\big)^T \quad (10)$$

$$A_{IF} = \big(P_j \cdot A_u \quad e_{2 \cdot j} \quad -\Lambda_j \otimes (P_j \cdot e_{2 \cdot n}) \\ P_j \cdot A_b \quad -\Lambda_j \otimes (P_j \cdot (e_2 \otimes \Lambda_2)) \quad P_j \cdot A_N\big) \quad (11)$$

$$X_{IF} = \begin{bmatrix} \Delta x_r^s & t_r & t^s & b_r & b^s & \tilde{N} \end{bmatrix}^T \quad (12)$$

The symbols l_{IF}, A_{IF}, and Z_{IF} denote the l-vector, design matrix, and the estimated parameters for the IF-PPP model, respectively.

The above two approaches have advantages and disadvantages. Although the first-order ionospheric effects in the IF-PPP approach are eliminated in the observation combination, the observation noises are amplified and IF-PPP is not suitable for single-frequency data. On the other hand, the PPP based on raw observations has the flexibility of

processing multi-frequency observations, but it requires estimation of ionospheric parameters.

Biases in multi-GNSS PPP models

In the IF-PPP models, the t^s in (8) and (12) is always eliminated by using the IGS precise clock products. In the PPP modes based on raw observations, bias terms are reintroduced in order to adopt the IGS precise clock products. Meanwhile, the receiver clock offsets and the biases at the receiver in GNSS PPP model must be considered. We also briefly present the ionospheric modeling approach.

IGS precise clock products and the satellite signal delay

It is noted that the satellite clock term t_f^s is linearly dependent on the signal delay b_f^s; hence, the signal delays are not separable from the satellite clock offset without additional constraints. As the IGS precise satellite clock products are estimated with the ionospheric-free observations, it involves the ionospheric-free combination of the signal delays b_1^s and b_2^s,

$$T_{IGS}^s = t^s + J \cdot \begin{pmatrix} b_1^s & b_2^s \end{pmatrix}^T \tag{13}$$

When using the IGS precise clock products, PPP users can directly eliminate the satellite clock offsets by using the same observation types as those adopted in the estimation of precise clock products with the IF-PPP approach, while the satellite signal delay needs to be corrected in addition to the satellite clocks to keep consistency when PPP based on raw observations is adopted or different observation types are used in the IF-PPP approach. Define the correction for each signal as b_i ($i = 1, 2, …, n$):

$$
\begin{aligned}
b_i &= J \cdot \begin{pmatrix} b_1^s & b_2^s \end{pmatrix}^T - b_i^s \\
&= \frac{f_1^2}{f_1^2 - f_2^2} \cdot (b_1^s - b_i^s) - \frac{f_2^2}{f_1^2 - f_2^2} \cdot (b_2^s - b_i^s)
\end{aligned}
\tag{14}
$$

Fortunately, IGS provides the products known as differential code biases (DCB) to correct for different code observations. PPP users can calculate b_i using the DCB products for correcting the clock offset using $T_{IGS}^s - b_i$. For example, with the IGS clock products using P1/P2 observations, the GPS (P1 and P2) signal delay is corrected as follows:

$$
\left.
\begin{aligned}
b_1^s &= f_2^2/(f_1^2 - f_2^2) & \mathrm{DCB_{P1P2}} \\
b_2^s &= f_1^2/(f_1^2 - f_2^2) & \mathrm{DCB_{P1P2}}
\end{aligned}
\right\}
\tag{15}
$$

where $\mathrm{DCB_{P1P2}}$ is provided by IGS DCB products.

Receiver-specific uncalibrated code delays (UCD)

The UCD for CDMA signals are identical for all satellites, but are different for receivers in case of FDMA signals. Because $b_{r,1}$ and $b_{r,2}$ in each GNSS system are linearly

dependent, the following constraint equations are added to overcome the datum deficiency in the equation systems:

$$
\begin{cases}
b_{r,1} = 0 & \mathrm{CDMA} \\
\sum_{i=0}^{j} b_{r,1}(i) = 0 & \mathrm{FDMA}
\end{cases}
\tag{16}
$$

$$\sum_{i=0}^{j} \left(J \cdot \begin{pmatrix} b_{r,1} & b_{r,2} \end{pmatrix}^T \right)(i) = 0 \tag{17}$$

where j is the number of GLONASS satellites in view.

In the IF-PPP model, the receiver clock offset can absorb the combination of UCD ($J \cdot \begin{pmatrix} b_{r,1} & b_{r,2} \end{pmatrix}^T$) for GNSS systems based on CDMA signals. However, an additional constraint is needed for GLONASS PPP to remove the datum deficiency as shown in (17).

Receiver clock offset

Considering the differences between the signals of different GNSS, the receiver can introduce the inter-system biases (ISB) for pseudorange and the carrier phase measurements (Dach et al. 2010). It can be explained as the differences between GNSS receiver clock offset as follows:

$$t_{r,sys} = t_{r,GPS} + \mathrm{ISB}(sys \neq \mathrm{GPS}) \tag{18}$$

There are two ways of handling ISB. The first method is that independent receiver clocks per GNSS are introduced (Choy et al. 2013). The second method is to treat the ISB as one constant or as piece-wise linear parameters (Cai and Gao 2013). The receiver clock error is the offset related to a single common reference time, e.g., GPS, GLONASS, BDS, or Galileo time, relative to the satellite clock products used (Choy et al. 2013). In this study, the first method is adopted and the receiver clock offsets are estimated as white noise.

Ionospheric delay

For the PPP with raw observations, an a priori ionospheric model is introduced as constraints as proposed by Shi et al. (2012),

$$
\left.
\begin{aligned}
I(z)_r^s &= a_0 + a_1 dL + a_2 dL^2 + a_3 dB + a_4 dB^2 + r_r^s \\
\tilde{I}(z)_r^s &= a_0 + a_1 dL + a_2 dL^2 + a_3 dB + a_4 dB^2 + r_r^s + \varepsilon_{I(z)_r^s}
\end{aligned}
\right\}
\tag{19}
$$

where a_i ($i = 0, 1, 2, 3, 4$) are the coefficients that describe the deterministic behavior of the ionospheric delay; the scalar field r_r^s, which includes the small features superimposed on the polynomial, represents the stochastic behavior; dL and dB are the longitude and latitude difference between the ionospheric pierce point (IPP) and the approximate location of station, respectively; $\tilde{I}(z)_r^s$ is the vertical ionospheric delay correction interpolated from

Global Ionosphere Map (GIM) or an available regional ionosphere model (Yao et al. 2013) with corresponding noise $\varepsilon_{\tilde{I}(z)_r^s}$.

Experimental results and performance analyses

The PPP based on raw observations are suitable for single-, dual-, or multi-frequency data processing and for multi-GNSS systems. We now perform comprehensive numerical analyses to demonstrate how the new PPP model with raw observations contributes to PPP computing and performance. In the following, we briefly describe the data sets and processing schemes first. Next we present the results with various computing schemes.

Data collection and processing schemes

The performance of single- and dual-frequency multi-GNSS PPP solutions are evaluated using data sets collected from the 105 MGEX stations as shown in Fig. 1 for July 2014. Of these stations, 55 stations can track BDS signals as shown in Fig. 3.

The DCB corrections depend on GNSS observation types. The new signal structures of GPS, BDS, and Galileo make it possible to generate code and phase observations based on one or a combination of two channels composed of I and Q components. For Galileo E5a, E5X (I + Q) and E5Q can be tracked in the MGEX network and about 75 MGEX stations can track E5X, which are used for our PPP performance evaluation with the Galileo system. The GPS observation C2W (based on Z-tracking and similar) is used in the model and performance evaluation. For detailed information on different GNSS signals, we refer to Gurtner (2013).

As an important factor in PPP performance, the Geometric Dilution of Precisions (GDOP) of each individual constellation are given. With the cutoff elevation of 7°, the GDOP are calculated every 15 min and averaged to show the geometry strength in different regions around the world. Figures 1, 2, and 3 plot the GDOP values against the tracking station locations for GPS, GLONASS, and BDS
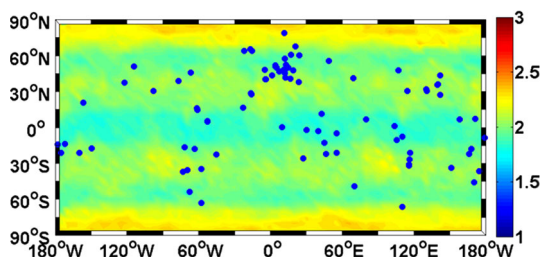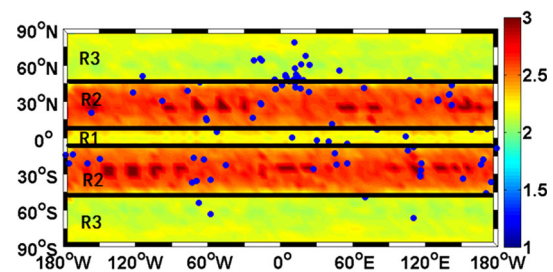

Fig. 2 GLONASS global GDOP and distribution of GLONASS track stations
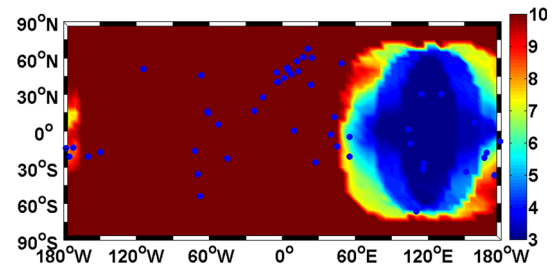

Fig. 3 BDS global GDOP and distribution of BDS track stations

constellations, respectively, for DOY 182 in 2014. The GDOP of Galileo constellation is not presented as it has only four satellites in orbit. The current BDS constellation only provides regional services, and areas with GDOP > 10 or with less than four BDS satellites in view are regarded as out of the navigation service region. It is concluded that the GPS GDOP distribution is fairly uniform, while the GLONASS GDOP in the high latitude regions is lower (better) than that in the mid-latitude regions. The BDS GDOP values in the Asia–Pacific region are small enough for positioning. In general, GPS GDOP values are between 1.5 and 2.5, while GLONASS GDOP values range from 2 to 3, and BDS GDOP values are over 3. The GDOP factors will have a direct impact on the PPP performance.

As BDS are still regional and Galileo has only four satellites, evaluation of the benefits of BDS or Galileo system on the multi-GNSS PPP is performed only when the number of BDS or Galileo satellites is three or more. The satellite system identifiers "G, R, C, E" as denoted in RINEX 3.02 format are used to represent GPS, GLONASS, BDS, and Galileo, respectively. For a combined system, all identifiers are combined to denote the combination of GNSS constellations; for example, GPS + GLONASS + BDS + Galileo is denoted as "GRCE." The parameters estimation strategy and model corrections in GNSS PPP are summarized in Table 1.

The PPP performance in terms of convergence time and position accuracy is evaluated at the 68 and 95 % confidence level in kinematic PPP mode. For dual-frequency

Fig. 1 GPS global GDOP and distribution of GPS track stations

Table 1 Strategies for multi-GNSS PPP

Parameters	PPP with raw observations
Observations	Raw observations
Sampling rate	30 s
Cutoff angle	7°
PCO/PCV	GPS and GLONASS PCO/PCV corrected with igs08.atx BDS and Galileo PCO corrected with the value released by IGS MGEX and PCV is not considered
Phase windup	Phase polarization effects applied (Wu et al. 1993)
Solid earth tides	IERS 2010
Troposphere	Saastamoinen model and GMF (Dach et al. 2007)
Ionosphere	Piece-wise for polynomials in 5 min and random walk for temporal variation (Shi et al. 2012), GIM as a priori information constraint
Receiver clock	Estimated as white noise for each GNSS system
UCD	Estimated as random walk for receiver UCD while the satellite UCD (DCB) corrected with CODE and MGEX

solutions, the convergence time is determined when the positioning accuracy is better than 0.2 m (95 %) and 0.1 m (68 %) in the horizontal and vertical directions, respectively. For single-frequency PPP solutions, the convergence time is determined when the positioning accuracy is better than 0.5 m (95 %) and 0.3 m (68 %) in the horizontal and vertical components, respectively. The position accuracy is presented for both horizontal and vertical components, and it is determined after convergence when the positioning error remains stable with time.

Results and analysis

Based on the results obtained from different schemes, the performance of IF-PPP and PPP based on raw observations is compared with single constellation first. Then, some characteristics of GLONASS and BDS PPP are discussed based on raw observations. Finally, the performance in convergence and accuracy of multi-GNSS PPP, including the single frequency and dual frequency, is analyzed.

Performance comparison of PPP with raw observations and IF-PPP solutions

As GPS, GLONASS, and BDS can independently provide navigation service around world or in Pacific–Asian region, the comparisons are made with each individual constellation with dual-frequency observations. Figure 4 shows the horizontal and vertical RMS values of two PPP solutions from different constellations, based on the statistics over all of the available MGEX stations. Note that the performance of the BDS PPP solutions is evaluated with MGEX stations within the Asian–Pacific region only. Table 2 presents the convergence time determined when the positioning error is
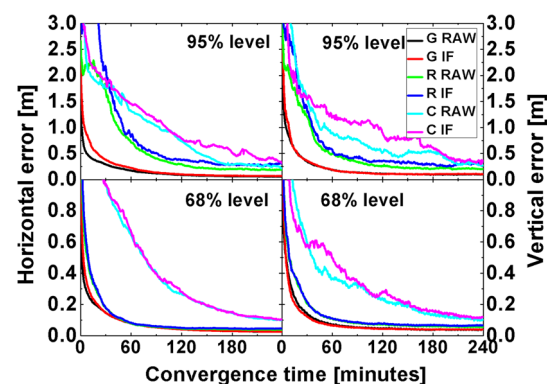

Fig. 4 Convergence performance of PPP based on raw observations and IF-PPP with single constellation

lower than 0.2 m (95 %) and 0.1 m (68 %) in the horizontal and vertical directions.

From Fig. 4 and Table 2, we can see that it takes 47 and 41.5 min for GPS PPP with raw dual-frequency measurements to converge to the defined 1σ accuracy in horizontal and vertical components, respectively. The convergence time for 2σ accuracy in both components is 51.5 and 56.5 min, respectively. On the other hand, GLONASS PPP requires the convergence time of 50 and 67.5 min to achieve the same 1σ accuracy. It is noted that neither GLONASS IF-PPP nor PPP based on raw observations can achieve the positioning accuracy of better than 0.2 m in vertical direction at the 95 % confidence level. The BDS dual-frequency PPP takes about 4 h or more to achieve the accuracy of 0.1 m at the 68 % level and does not converge in the vertical direction at the 2σ level.

Table 3 summarizes the PPP positioning accuracy after convergence with the two PPP approaches for these three systems. The PPP solutions based on raw observations

Table 2 Convergence time of PPP with raw observations and IF-PPP solutions

	PPP with raw observations (min)				IF-PPP (min)			
	H (95 %)	H (68 %)	V (95 %)	V (68 %)	H (95 %)	H (68 %)	V (95 %)	V (68 %)
G	51.5	47	56.5	41.5	65.5	47	58	36.5
R	163.5	50	–	67.5	–	52	–	69
C	257	239	–	236	240	230.5	–	251.5

Table 3 Accuracy comparison of PPP based on raw observations and IF-PPP

	PPP based on raw observations (cm)				IF-PPP (cm)			
	H (95 %)	H (68 %)	V (95 %)	V (68 %)	H (95 %)	H (68 %)	V (95 %)	V (68 %)
G	5.88	2.55	10.13	3.82	6.83	2.63	10.66	3.94
R	19.06	3.92	20.90	5.72	28.78	4.54	30.30	6.50
C	10.99	4.48	21.74	8.66	11.28	4.63	22.77	9.55

show some advantages over the IF-PPP solutions which are more evident with the GLONASS constellation at the 95 % level. The IF-PPP positioning performance degradation is mainly caused by the noise amplification when using the ionospheric-free combinations. Overall, as expected the positioning accuracy with GPS is the best among all the three systems in terms of the convergence time and accuracy. BDS PPP can achieve an accuracy of better than 5 and 10 cm in the horizontal and the vertical direction at the 68 % level, which is slightly worse than the GLONASS PPP positioning performance. However, at 95 % level, the positioning accuracy of BDS is better than that of GLONASS PPP in most of the cases. It is generally believed that the convergence time performance of the PPP solution based on raw observations depends on an a priori knowledge of the ionosphere model. It can take advantage of a high-accuracy ionosphere model to realize better convergence performance as suggested by Juan et al. (2012) and Banville et al. (2014), while the IF-PPP solution does not offer this advantage.

From the above comparison, it is noted that the PPP based on raw observations with prior ionospheric constraint shows better performance than IF-PPP. Hence, in the following the PPP performance is analyzed based on raw observations, and the term "PPP" means PPP based on raw observations without specific explanation.

Performance of single-frequency PPP with single constellations

The single-frequency PPP convergence and accuracy with GPS, GLONASS, and BDS systems are shown in Fig. 5 and Table 4, respectively. It is seen that only GPS single-frequency PPP solutions can reach the defined convergence criteria, i.e., accuracy of better than 0.5 m at the 95 % level and 0.3 m at the 68 % level in both horizontal and vertical
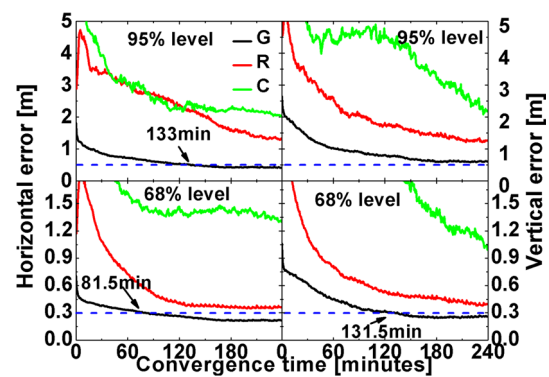

Fig. 5 Illustration of convergence of single-frequency PPP solutions with raw observation models

Table 4 Single-frequency PPP positioning accuracy after convergence (m)

	GPS	GLONASS	BDS
H (95 %)	0.42	1.35	1.34
H (68 %)	0.22	0.36	0.70
V (95 %)	0.60	1.26	1.51
V (68 %)	0.26	0.40	0.84

directions. Similarly to the dual-frequency PPP results, GPS single-frequency PPP outperforms in both the convergence time and the positioning accuracy. The single-frequency BDS PPP solutions show worse performance than that of GLONASS PPP.

A number of factors can contribute to the worse performance of single-frequency GLONASS and BDS PPP solutions as compared to GPS. The larger GDOP value is certainly one key factor. In the case of GLONASS FDMA signals, the satellite-specific IFB at the receiver is strongly
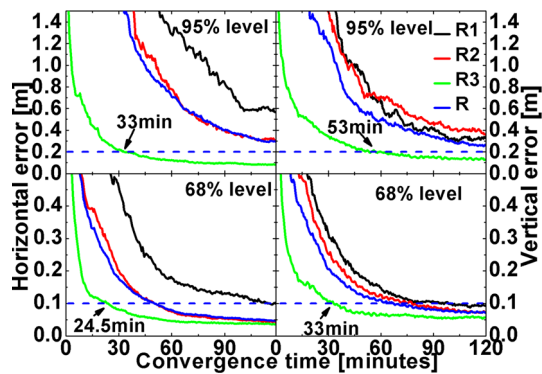
Fig. 6 Convergence performance of GLONASS dual-frequency PPP in different latitude regions
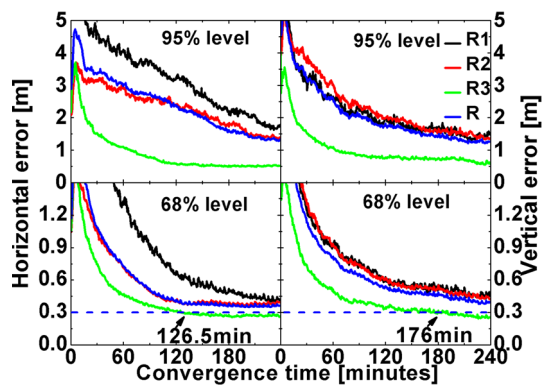

Fig. 7 Convergence performance of GLONASS single-frequency PPP in different latitude regions

correlated with the ionosphere. As for BDS, the pseudorange measurements show elevation-dependent variation that depends on frequencies and satellite types such as GEO, IGSO, and MEO (Wanninger and Beer 2015).

Performance of GLONASS PPP in different regions

The GLONASS GDOP in Fig. 2 shows evident regional characteristics, which could have an impact on the PPP performance for GLONASS constellation. The GLONASS PPP performance is analyzed against the station located in regions marked R1, R2, and R3 in Fig. 2. The average

number of stations spread in the R1, R2, and R3 region is 19, 47, and 39, respectively.

Figures 6 and 7 show the dual- and single-frequency GLONASS PPP convergence performance in the three regions. Both single- and dual-frequency PPP solutions demonstrate shorter convergence time in the higher latitude regions. This is especially the case for the vertical component. It is noted that the convergence performance of GLONASS dual-frequency PPP at the high latitude region (R3) is even better than the GPS dual-frequency PPP. For instance, it only takes 24.5 min for the GLONASS PPP to achieve the horizontal accuracy of better than 0.1 m at the 68 % level. The convergence time reduction over GPS is 48 % and 20 % in the horizontal and the vertical component, respectively. However, the GLONASS single-frequency PPP in the R3 region is still worse than GPS due to the effects of IFB as discussed. The positioning accuracy after convergence in different regions is summarized in Table 5. Similarly to the convergence performance, both the GLONASS dual- and single-frequency PPP positioning accuracies increase in the high latitude areas, but the overall positioning accuracy in the high latitude region (R3) is still lower than the GPS accuracy.

The GPS and GLONASS are often coupled together to provide better positioning services. Hence, the impacts of GLONASS regional characteristics on the PPP performance are of interest. The combined GPS/GLONASS PPP convergence in terms of different regions R1, R2, and R3, as shown in Fig. 2, denoted by GR1, GR2, and GR3 and the global MGEX stations (denoted by GR) are illustrated in Figs. 8 and 9 for the dual- and single-frequency cases, respectively. The positioning accuracy after convergence in different regions is given in Table 6. Compared to the GPS-only PPP, both the single-frequency GR convergence time and dual-frequency GR convergence time improve by about 50 % at both the 68 and 95 % levels. The single-frequency PPP accuracy after convergence improves by 25 % at 95 % level and 16 % at the 68 % level with respect to GPS-only PPP. However, the dual-frequency PPP accuracy exhibits insignificant accuracy improvement after convergence. Overall, the combined GPS/GLONASS positioning performances at the high latitude region (GR3) is still better than GR1 and GR2, although the

Table 5 GLONASS PPP positioning accuracy after convergence in different regions

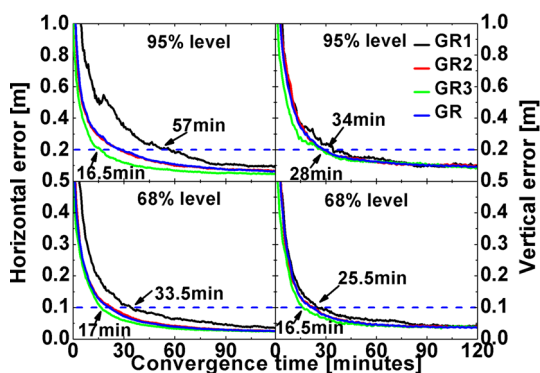|	Dual-frequency PPP (m)				Single-frequency PPP (m)			
	H (95 %)	H (68 %)	V (95 %)	V (68 %)	H (95 %)	H (68 %)	V (95 %)	V (68 %)
R	0.19	0.04	0.21	0.06	1.35	0.36	1.26	0.40
R1	0.25	0.06	0.32	0.08	1.51	0.33	1.73	0.43
R2	0.22	0.04	0.25	0.05	1.04	0.30	1.23	0.41
R3	0.07	0.03	0.14	0.05	0.52	0.27	0.63	0.26

Fig. 8 Convergence performance of dual-frequency PPP (GPS + GLONASS) in different regions
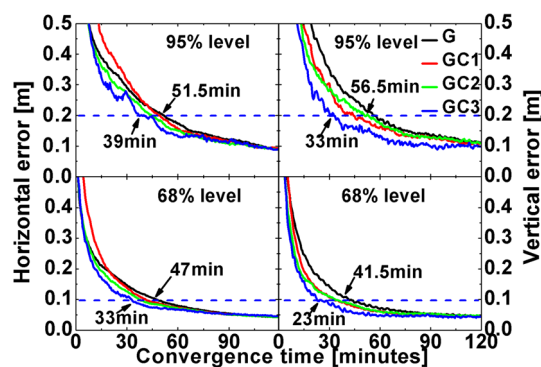

Fig. 10 Convergence performance of dual-frequency PPP (GPS + BDS) in different regions
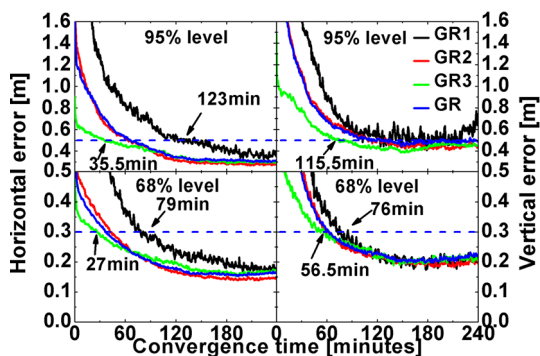

Fig. 9 Convergence performance of single-frequency PPP (GPS + GLONASS) in different regions
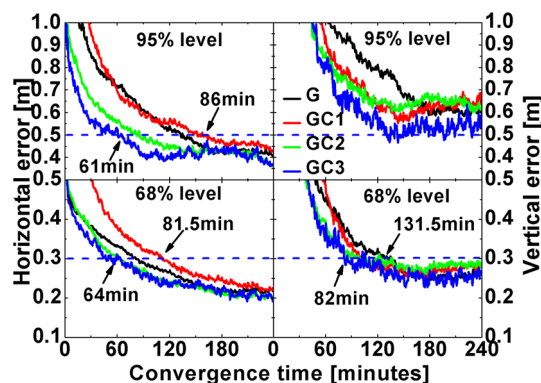

Fig. 11 Convergence performance of single-frequency PPP (GPS + BDS) in different regions

improvement is not as evident as shown in the GLONASS-only case. This implies that the advantage of the GLONASS in high latitude regions on the PPP performance is no longer significant as a result of complementary GPS and GLONASS combination. It is expected that the multi-GNSS PPP will further eliminate the regional differences such that the homogenous performance can be expected everywhere on the earth surface.

Performance of GPS/BDS PPP

As BDS consists of three orbit types including GEO, IGSO, and MEO, the effects of GEO satellites on the PPP convergence and positioning performance are less understood.

Since there are not enough satellites in view for analysis of the PPP performance without the GEO satellites, we compare the performance of the combined GPS/BDS PPP with all BDS satellites (referred to as GC1) and the combined GPS/BDS PPP without BDS GEO satellites, i.e., GPS + BDS IGSO + BDS MEO (referred to as GC2). Furthermore, as the BDS is currently providing regional service, the combined GPS/BDS PPP performance without BDS GEO satellites is studied only in the Asia–Pacific region (referred to as GC3). The single- and dual-frequency PPP convergence results for GPS (G), GC1, GC2, and GC3 are illustrated in Figs. 10 and 11, respectively.

Table 6 GPS/GLONASS PPP positioning accuracy after convergence in different cases

	Dual-frequency PPP (unit cm)				Single-frequency PPP (unit m)			
	H (95 %)	H (68 %)	V (95 %)	V (68 %)	H (95 %)	H (68 %)	V (95 %)	V (68 %)
GR	6.90	2.71	9.72	3.76	0.31	0.16	0.49	0.22
GR1	6.02	2.39	11.45	4.37	0.32	0.15	0.51	0.20
GR2	5.09	2.12	8.95	3.66	0.29	0.14	0.51	0.21
GR3	4.45	2.18	10.26	3.45	0.30	0.17	0.53	0.21

Table 7 GPS/BDS PPP positioning accuracy after convergence

	Dual-frequency PPP (unit cm)				Single-frequency PPP (unit m)			
	H (95 %)	H (68 %)	V (95 %)	V (68 %)	H (95 %)	H (68 %)	V (95 %)	V (68 %)
G	5.99	2.56	10.10	3.86	0.42	0.22	0.60	0.20
GC1	7.34	2.97	10.35	4.35	0.45	0.23	0.65	0.28
GC2	6.77	2.88	10.23	4.23	0.40	0.20	0.63	0.29
GC3	7.13	3.07	9.03	3.86	0.39	0.21	0.55	0.26

The combined PPP has shown a somewhat significant convergence improvement over the GPS-only PPP when the BDS GEO satellites are excluded, i.e., in the GC2 and GC3 cases. The impacts of GEO satellites in the GC1 case are positive to the vertical component in both single- and dual-frequency PPP cases but are negative to the horizontal component of the single- and dual-frequency PPP. Furthermore, results of the regional case (GC3) have shown slight improvements over the GC2 case which is as expected due to the additional IGSO satellites that are available in the region.

Table 7 summarizes the positioning accuracy of the GPS/BDS combined PPP after-convergence solutions. Among all the GPS/BDS combined PPP cases, the positioning accuracy has shown very similar improvement as the convergence time when the BDS GEO satellites are removed. The GC1 case including the BDS GEO satellites shows the worst positioning accuracy in both dual- and single-frequency PPP solutions. The BDS GEO satellites have negative effects on the GPS/BDS combined PPP positioning accuracy as well. Furthermore, compared with the GPS-only PPP performance, the combined GPS/BDS positioning accuracy is not necessarily better in any of the three cases. This may be because the accuracy of BDS satellite precise products is clearly lower than those of GPS.

This phenomenon is different from the GLONASS results where the convergence and positioning accuracy improve with the decrease in GDOP value. The combined GPS/BDS PPP gives better results by dropping the observations of BDS GEO satellites. The main reason is the low GEO orbit accuracy (Lou et al. 2014) and the large multipath effect (Schempp et al. 2008). In this case of having enough satellites for positioning, the BDS GEO satellites may be excluded in multi-PPP data processing until the GEO orbits and clocks products are sufficiently improved and their measurements can make positive impacts.

Performance of PPP with multi-GNSS constellations

The PPP performance was evaluated with both the raw single- and dual-frequency data in various multi-GNSS configurations, including GRC, GRE, and GRCE. As the influence of the GLONASS regional characteristics in
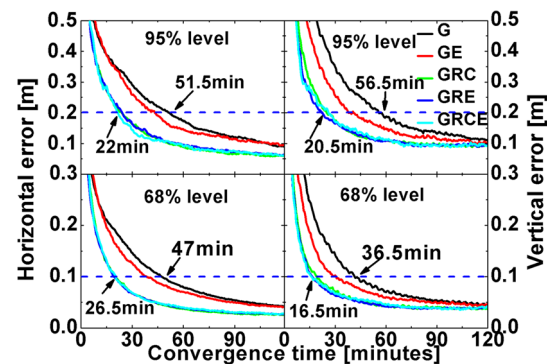
Fig. 12 Convergence performance of multi-GNSS dual-frequency PPP

multi-GNSS configurations has been understood, no special consideration is given with respect to the station location when including GLONASS in the evaluation. On the other hand, the BDS GEO satellites are excluded in the evaluation due to their understood impact on the PPP performance. In addition, four Galileo IOV satellites are included in the analysis.

Figure 12 shows the greatly improved convergence performance of multi-GNSS dual-frequency PPP solutions compared to the GPS-only results. The improvement of approximately 63 and 61 % for the horizontal and vertical components at the 68 % level and 57 and 44 % for the horizontal and vertical components at the 95 % level is exhibited. With only three Galileo IOV satellites (E20 is not available), the GPS/Galileo combined dual-frequency PPP (GE) convergence time can be reduced by about 15 min at the 95 % level. It is noted that the contribution of Galileo to the vertical solution is more significant than to the horizontal direction. Figure 13 illustrates the convergence improvement of the multi-GNSS single-frequency PPP comparing to the GPS-only results. Overall, the GRE combination results in the best convergence performance out of the GRC and GRCE combinations. As the BDS pseudorange measurements are more affected by the elevation-dependent bias (Wanninger and Beer 2015), it is challenging to adequately handle the stochastic models in the multi-GNSS environments. This could most likely be the cause of the degraded convergence performance of the GRC and GRCE single-frequency PPP results. Overall, the
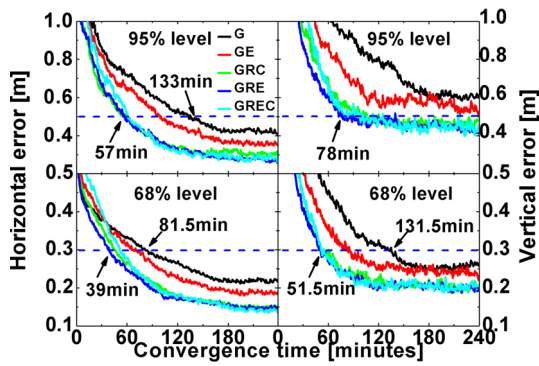
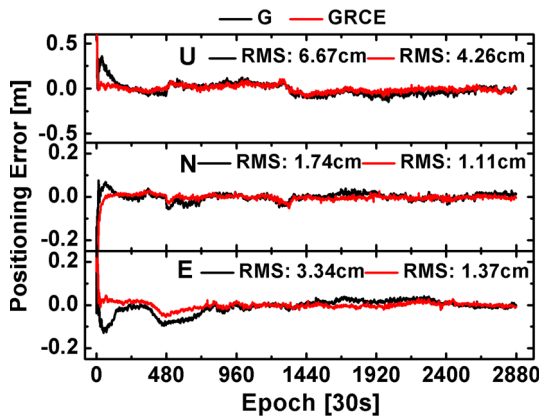Fig. 13 Convergence performance of multi-GNSS single-frequency PPP

Fig. 14 MGEX station MRO1 dual-frequency PPP error time series
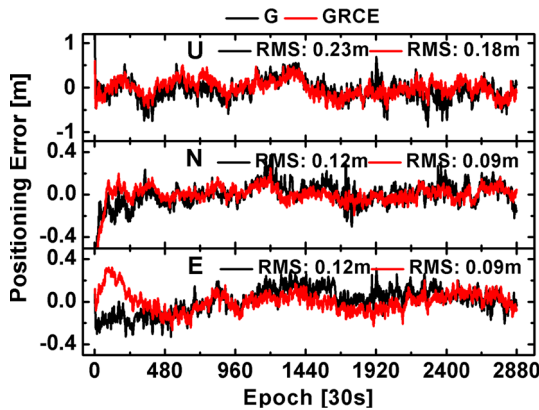

Fig. 15 MGEX station MRO1 single-frequency PPP error time series

multi-GNSS PPP convergence time can be reduced to less than 60 and 30 min for the single- and dual-frequency PPP solutions, respectively.

In addition to the combined PPP convergence performance, the accuracy after convergence in different cases is compared in the following. Figures 14 and 15 present the dual- and single-frequency kinematic PPP time series of
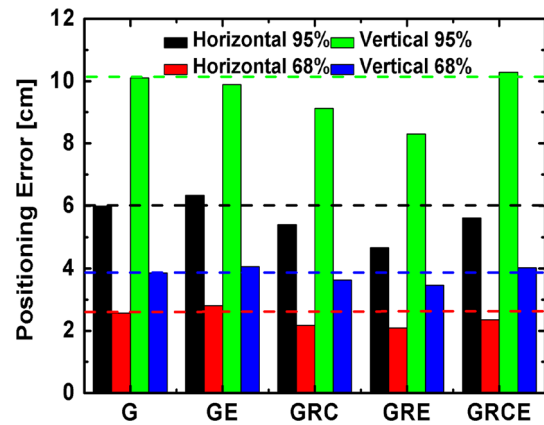

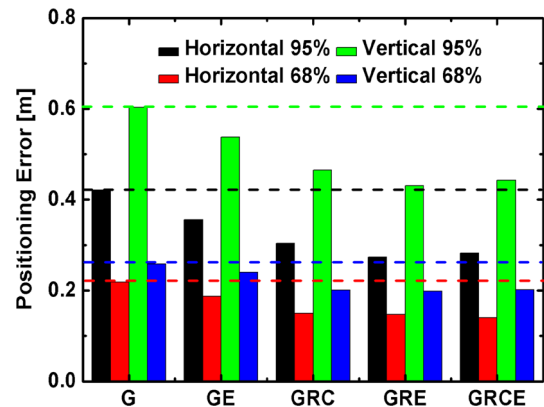Fig. 16 Dual-frequency PPP accuracy after convergence in different cases

Fig. 17 Single-frequency PPP accuracy after convergence in different cases

the MGEX MRO1 station obtained on DOY 183, 2014. The kinematic PPP results with the GPS-only and multi-GNSS (GRCE) environment are shown in black and red lines, respectively. The multi-GNSS PPP clearly shows better accuracy reliability than the GPS-only. The positioning RMS (exclude first 10 min) improves by about 40 and 25 % in dual-frequency and single-frequency cases, respectively, in both the horizontal and vertical directions.

The kinematic PPP positioning performance of the 105 MGEX stations over the month of July 2014 is plotted in Figs. 16 and 17 for the dual and single frequency, respectively. It is observed that the GE dual-frequency PPP exhibits slightly worse performance than the GPS-only PPP. This is mainly because the positioning accuracy after convergence is more dependent on the accuracy of the orbit and clock solutions. The uncertainty of the current Galileo orbit and clock solutions is at the decimeter level (Steigenberger et al. 2015), which may have outweighed the benefits of having a few additional Galileo satellites. With more satellites available, GRC, GRE, and GRCE

cases have all shown improvements of approximately 15 %. Similar to the convergence results, the GRE positioning performance is better than the GRC and GRCE, which indicated the negative impacts of elevation-dependent bias in the BDS pseudorange measurements. Similarly, the single-frequency multi-GNSS PPP positioning accuracy has shown improvements of 10–30 % in the horizontal and vertical components, compared to the GPS results.

Overall, the multi-GNSS kinematic PPP without ambiguity resolution has shown the accuracy of better than 3 cm in the horizontal and 4 cm in the vertical components at the 68 % level (1σ). For single-frequency PPP, better and more reliable accuracy can be achieved with more observations used. GPS single-frequency PPP can achieve the accuracy of 0.22 and 0.26 m in the horizontal and vertical component (1σ), respectively. For multi-GNSS combined cases, the accuracy of better than 0.2 m in the horizontal and vertical can be obtained at the 68 % level (1σ).

Conclusions

This study has presented the GNSS PPP model for the raw observations with consideration of signal delay biases and the ionospheric delay. The model is generally suitable for single-, dual-, or multi-frequency data processing and for multi-GNSS systems. Comprehensive numerical analyses have been performed with the one month data collected from 105 MGEX stations. The PPP results based on undifferenced or raw observations have shown the overall better convergence and positioning accuracy performance than the IF-PPP results. The comparison has been made using dual-frequency data sets with each single constellation of GPS, GLONASS, or BDS. Overall, the PPP performance for GPS outperforms the GLONASS and BDS systems in both the single- and dual-frequency data cases. This is mainly due to the pseudorange measurement issues that exist in the GLONASS system in the form of strong correlation between IFB and ionosphere, and in the BDS system in the presence of elevation-dependent variations. The higher GDOP value for BDS and GLONASS constellation is another important factor.

The GLONASS PPP performance has shown obvious regional characteristics relating to the satellite geometry (GDOP). The convergence performance and positioning accuracy are better in the higher latitude areas and could provide better performance than GPS in the high latitude region with the dual-frequency data. However, due to the effect of IFB, GLONASS single-frequency results do not achieve the same precision as GPS. In the combined GPS/GLONASS PPP solutions, the performance impact is much smaller than the GLONASS-only case. It is anticipated that the impact will be further negligible in multi-GNSS environment such that the same performance can be expected anywhere around the world.

Although the BDS-only PPP result shows the worse performance with respect to GPS and GLONASS, the combined GPS/BDS result shows a largely reduced convergence time if the BDS GEO satellites are excluded in the computation. However, the positioning accuracy of the combined GPS/BDS is not necessarily better than the GPS accuracy, due to the uncertainty of BDS precise orbits and clock solutions at the decimeter level. Additionally, it is noted that the combined GPS/BDS results show the best performance in the Asian–Pacific region which is in the coverage of the current BDS service.

With multi-GNSS combined dual-frequency PPP, the convergence has been significantly improved, while the positioning accuracy after convergence has shown no significant improvement. The four-system (GRCE) combined results have shown improvement in the convergence time by more than 60 % in both the single- and dual-frequency cases when comparing with the GPS-only results, while the positioning accuracy after convergence has no significant improvements. As far as the multi-GNSS single-frequency PPP is concerned, both the convergence and positioning accuracy have demonstrated improvement. Results have shown that the global positioning accuracy of better than 0.3 m in the horizontal can be obtained within 40 min and the positioning error of better than 0.2 m in the horizontal and vertical directions after convergence can be achieved.

The research has shown the performance benefits that the multi-GNSS can offer to PPP with the current constellations. For greater potential and higher-performance benefits of multi-GNSS expectable in the future, we have also identified some limiting factors that need to be further investigated. First, the current BDS and Galileo precise orbit and clock solution only offers decimeter level of accuracy and needs to be further improved such that all the GNSS systems are defined in an identical reference frame with similar accuracy. Second, the elevation-dependent bias of the BDS pseudorange has shown an impact on the BDS positioning performance and needs to be investigated. Third, the BDS GEO satellites are shown to have negative impacts on the PPP performance. Apart from the poor orbit and clock solution, there might exist other types of biases or bias variation that need to be further investigated. Finally, GPS, BDS, and Galileo systems are offering three or more frequency signals, which could bring further improvements to the PPP based on raw observations.

References

Banville S, Collins P, Zhang W, Langley RB (2014) Global and regional ionospheric corrections for faster ppp convergence. Navigation 61(2):115–124

Cai C, Gao Y (2007) Precise point positioning using combined GPS and GLONASS observations. J Glob Position Syst 6(1):13–22

Cai C, Gao Y (2013) Modeling and assessment of combined GPS/GLONASS precise point positioning. GPS Solut 17(2):223–236

Choy S, Zhang S, Lahaye F, Héroux P (2013) A comparison between GPS-only and combined GPS + GLONASS precise point positioning. J Spat Sci 58(2):169–190

Chuang S, Wenting Y, Weiwei S, Yidong L, Rui Z (2013) GLONASS pseudorange inter-channel biases and their effects on combined GPS/GLONASS precise point positioning. GPS Solut 17(4):439–451

Dach R, Hugentobler U, Fridez P, Meindl M (2007) Bernese GPS software version 5.0. Astronomical Institute, University of Bern, 640, 114

Dach R, Schaer S, Lutz S, Meindl M, Beutler G (2010) Combining the observations from different GNSS. In: EUREF 2010 symposium, pp 02–05

Defraigne P, Baire Q (2011) Combining GPS and GLONASS for time and frequency transfer. Adv Space Res 47(2):265–275

Dow JM, Neilan RE, Rizos C (2009) The international GNSS service in a changing landscape of global navigation satellite systems. J Geod 83(3–4):191–198

Ge M, Zhang H, Jia X, Song S, Wickert J (2012) What is achievable with current COMPASS constellations? In: Proceedings of the ION GNSS 2012. Institute of Navigation, Nashville, TN, pp 331–339

Gu S, Shi C, Lou Y, Liu J (2015) Ionospheric effects in uncalibrated phase delay estimation and ambiguity-fixed PPP based on raw observable model. J Geod 89(5):447–457

Gurtner W, Estey L (2013) RINEX: the receiver independent exchange format, version 3.02, Technical Report, IGS Central Bureau

Hackel S, Steigenberger P, Hugentobler U, Uhlemann M, Montenbruck O (2013) Galileo orbit determination using combined GNSS and SLR observations. GPS Solut 19(1):15–25

Juan JM, Sanz J, Hernández-Pajares M, Samson J, Tossaint M, Aragón-Àngel A, Salazar D (2012) Wide area RTK: a satellite navigation system based on precise real-time ionospheric modelling. Radio Sci 47, RS2016. doi:10.1029/2011RS004880

Le AQ, Tiberius C (2007) Single-frequency precise point positioning with optimal filtering. GPS Solut 11(1):61–69

Li M, Qu L, Zhao Q, Guo J, Su X, Li X (2014) Precise point positioning with the BeiDou navigation satellite system. Sensors 14(1):927–943

Lou Y, Liu Y, Shi C, Yao X, Zheng F (2014) Precise orbit determination of BeiDou constellation based on BETS and MGEX network. Sci Rep 4, Article number: 4692

Monge BM, Rodríguez-Caderot G, de Lacy MC (2014) Multifrequency algorithms for precise point positioning: MAP3. GPS Solut 18(3):355–364

Montenbruck O, Hauschild A, Steigenberger P (2014) Differential code bias estimation using multi-GNSS observations and global ionosphere maps. Navigation 61(3):191–201

Schempp T, Burke J, Rubin A (2008) WAAS benefits of GEO ranging. In: Proceedings of the ION GNSS 2008, Institute of Navigation, Savannah, GA, 16–19 September, pp 1903–1910

Schönemann E, Becker M, Springer T (2011) A new approach for GNSS analysis in a multi-GNSS and multi-signal environment. J Geod Sci 1(3):204–214

Shi C, Gu S, Lou Y, Ge M (2012) An improved approach to model ionospheric delays for single-frequency precise point positioning. Adv Space Res 49(12):1698–1708

Steigenberger P, Hauschild A, Montenbruck O, Rodriguez-Solano C, Hugentobler U (2013) Orbit and clock determination of QZS-1 based on the CONGO network. Navigation 60(1):31–40

Steigenberger P, Hugentobler U, Loyer S, Perosanz F, Prange L, Dach R, Montenbruck O (2015) Galileo orbit and clock quality of the IGS multi-GNSS experiment. Adv Space Res 55(1):269–281

Tu R, Ge M, Zhang H, Huang G (2013) The realization and convergence analysis of combined PPP based on raw observation. Adv Space Res 52(1):211–221

Wanninger L, Beer S (2015) BeiDou satellite-induced code pseudorange variations: diagnosis and therapy. GPS Solut 19(4):639–648

Wu JT, Wu SC, Hajj GA, Bertiger WI, Lichten SM (1993) Effects of antenna orientation on GPS carrier phase. Manuscr Geod 18:91–98

Yang Y, Li J, Xu J, Tang J, Guo H, He H (2011) Contribution of the compass satellite navigation system to global PNT users. Chin Sci Bull 56(26):2813–2819

Yao Y, Zhang R, Song W, Shi C, Lou Y (2013) An improved approach to model regional ionosphere and accelerate convergence for precise point positioning. Adv Space Res 52(8):1406–1415

Zhao Q, Guo J, Li M, Qu L, Hu Z, Shi C, Liu J (2013) Initial results of precise orbit and clock determination for COMPASS navigation satellite system. J Geod 87(5):475–486

Yidong Lou is currently a professor at GNSS Research Center, Wuhan University. He received his Ph.D. in Geodesy and Surveying Engineering from the Wuhan University in 2008. His current research interest is in the real-time precise GNSS orbit determination and real-time GNSS PPP.
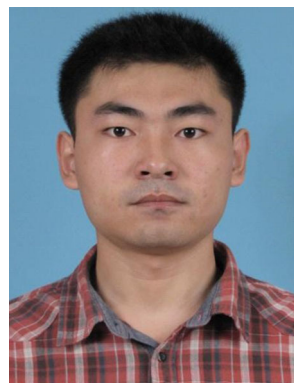
Fu Zheng is currently a Ph.D. student at GNSS Research Center, Wuhan University. He received his Master's degree at Wuhan University in 2015. His current research mainly focuses on multi-frequency GNSS PPP.

Shengfeng Gu is currently a postdoctoral researcher at Wuhan University. He received his Ph.D. from GNSS Research Center of Wuhan University. His current research mainly focuses on multi-GNSS data processing, PPP-RTK, and real-time ionosphere modeling.

Yanming Feng received his Ph.D. degree in satellite geodesy from Wuhan Technical University of Surveying and Mapping (Wuhan University, since 2000), China. He is currently a professor at School of Electrical Engineering and Computer Science, Queensland University of Technology, Australia. His research interests mainly include satellite orbit determination, multiple GNSS data processing algorithms, and precise GNSS positioning algorithms and applications.

Dr. Charles Wang is a Research Fellow in the Science and Engineering Faculty of Queensland University of Technology (QUT), Australia. His major research interests are in GNSS data processing, GNSS orbit estimation, network RTK precise positioning, and precise positioning for emerging applications. He is also a managing editor for Journal of Global Positioning Systems.

Hailin Guo is a Master Student at GNSS Research Center, Wuhan University. He received his Bachelor's degree at School of Geodesy and Geomatics in Wuhan University in 2015. His current research mainly focuses on PPP algorithm on handheld receiver.